1) 40

Ultraviolet Properties of Individual Hot Stars in Globular Cluster Cores. I. NGC 1904 (M 79)

Bruce Altner
Applied Research Corporation
Landover, MD 20785

Terry A. Matilsky
Rutgers University
Piscataway, NJ 08855-0849

Semi-annual Status Report
NASA Grant NAG5-1750
Prof. Terry Matilsky : P.I.
Rutgers University

ABSTRACT

As part of an observing program using the International Ultraviolet Explorer (IUE) satellite to investigate the ultraviolet properties of stars found within the cores of galactic globular clusters with blue horizontal branches (HBs), we obtained three spectra of the cluster NGC 1904 (M 79). All three were long integration-time, short-wavelength (SWP) spectra obtained at the so-called "center-of-light" and all three showed evidence of multiple sources within the IUE large aperture ($21''.4 \times 10''$). In this paper we shall describe the analysis of these spectra and present evidence that the UV sources represent individual hot stars in the post-HB stage of evolution. **Describe results of UV star extraction.** Analyses of other clusters observed as part of this same program will be discussed in a series of subsequent papers.

OMIT ?

1. Introduction

IUE observations of globular clusters with the SWP camera are equivalent to probes of their blue HB and UV-bright stars, since the cooler red giants contribute very little to the integrated light shortward of 1800 Å (deBoer and Code 1981). Code (1982) estimated that it would require almost 1000 red giants to equal the output of a single blue HB star at 1550 Å, based on the population synthesis models of Welch and Code (1980). In those clusters for which visual photometry exists in the core region, the IUE spectra therefore affords one the opportunity to improve upon the stellar atmosphere parameters (such as T_{eff}) derived from the optical data, as demonstrated by Aurière and Cordoni (1983) for two stars in M 15. In addition, IUE may also serve as a discovery instrument, as in the case of a spectrum of the core of M 13 which revealed a pair of *previously unknown* hot HB stars (de Boer and Code 1981). From that spectrum the authors were able to provide estimates of the effective temperatures and gravities of the two stars. Since there are relatively few IUE observations of hot Population II stars (only 7 of the 36 field stars in the Cacciari (1985) atlas are bluer than B-V = 0.2) such observations as those in M 15 and M 13 are quite important to our understanding of the evolutionary status of these stars, as well as their contribution to the integrated cluster light. We present below an analysis of another cluster (M 79) containing hot Population II stars, at least one of which seems to be a "supra-HB" object.

As a result of their investigation of 27 galactic globular clusters with the ANS satellite, van Albada, de Boer, and Dickens (1981) classified M 79 as an "extremely blue" (EB) cluster, signifying the presence of a large UV excess in the integrated light. It was also found to be a low-luminosity x-ray source, based on data from the IPC instrument on the Einstein X-ray Observatory (Grindlay 1981). However, no position of the x-ray source was given. Radial variation of B-V, as determined from a photometric survey of 161 stars in a $1' \times 1'$ field centered on the core by Cordoni and Aurière (1983), shows slight evidence of a color gradient (bluer toward the center), which the authors attribute to a "relatively random increase in the density of bright red giants" in the outer annuli. Gratton and Ortolani (1986) found two blue stars ($B - V \leq 0.$) at $V \sim 19$. Due to the high galactic latitude of M 79, it is unlikely that these stars are part of the galactic foreground, so

IUE IMAGES OF NGC 1904

IMAGE SWP	YEAR	DAY	EXPOSURE (minutes)	PA[1]	POINTING[2] h m s	° ′ ″	FOCUS STEP
25303[3]	1985	54	345	327.9	5 22 7.9	-24 34 10.4	-2.64
28936	1986	230	385	140.9	5 22 7.6	-24 34 10.3	-1.97
33152	1988	84	540	349.6	5 22 7.4	-24 34 10.0	-3.30

Table 1: Astrophysical Parameters for the Globular Clusters. [1] Position angle of large aperture, measured eastward from north. [2] RA and DEC (±2″) based on satellite maneuvers from offset star SAO 170395 (see Appendix A). [3] SWP 25303 has been reprocessed to take full advantage of the superior spatial resolution of the extended line-by-line image processing.

they may represent an extension to the BHB, as observed in other clusters (see *e.g.*, , Buananno *et al.* 1986). M 79 was observed by the Ultraviolet Imaging Telescope (UIT) during the ASTRO Spacelab mission in December, 1990 (Hill *et al.* 1991), using both the far-UV (1520 Å) and near-UV (2500 Å) bandpasses. The derived UV color magnitude diagram for 100 stars between 40″ and 5′ confirms both the presence of an extended BHB and the EB classification. Apparently, they have also detected individual giants in the UV. The UIT data shows stars both hotter than those picked up in visual surveys and hotter than those predicted by models of Sweigart (1987), suggesting that extreme mass loss has occurred in these stars, leaving them with almost negligible envelope masses.

2. Observations

We obtained long-exposure SWP spectra of M 79 with the IUE on three separate occasions, each time using the FES cursor to find the cluster's "center-of-light" (see Table 1 and Figure 1). As we show in the Appendix, the center-of-light in centrally condensed clusters such as M 79 is a well-defined and reproducible position. The coordinates derived from spacecraft slews for each observation are listed in the table, and demonstrate that the same field was observed in each case.

The position angle of the IUE large aperture for each of the three observations is nearly the same (with that of the second spectrum, SWP 28936, being rotated almost 180° with respect to the other two), suggesting again that many of the stars discussed below were observed on all three occasions. As discussed in Altner (1989) the spatial profiles derived from the IUE line-by-line (LBL) data are actually projections of the true stellar distribution along the long axis of the aperture.

Being long exposure-time observations, the SWP spectra are peppered with stray "hits", due to interaction of the camera phosphor with cosmic rays. In the subsequent reductions, data points so

affected have been removed. Other factors beside the background radiation have potential impact on image quality. One of the most important of these is the thermal environment. This affects the telescope focus, which is controlled by means of heaters near the primary mirror and on the camera deck. The unit of measure of telescope focus is the so-called focus "STEP"; Cassatella, Barbero, and Benvenuti (1985; hereafter CBB) have shown that optimum focus conditions prevail for STEP < 0 for the SWP camera. Under certain conditions the heaters fail to stabilize the focus properly and after several hours it may deteriorate to the point of causing an increase of 20–30% in the width of a spectrum (Sonneborn *et al.* 1987*a*). Since much our work on the globular cluster center-of-light images involves extraction of the spatially resolved spectra, we were always concerned with the possibility that less than optimum focus might cause a source in the aperture to appear broadened. For this reason, we include in Table 1 the value of the focus "STEP" parameter for each spatially resolved image analyzed in this paper.

3. Analysis

Two "non-standard" procedures, POLYSTAR and APS, are used in the bulk of the data reduction and analysis effort in this program. In this section we shall describe the motivation and logic behind both procedures, as well as their inherent errors, uncertainties and limitations.

a) POLYSTAR

Although the dramatic pictures one often sees of globular clusters leave the impression that even a fairly small aperture placed at the center would literally be filled with stars, such pictures are often intentionally overexposed in order to include the outer regions of the cluster. Shorter exposures reveal that the cluster core is composed of individual stars which are often distributed in a "patchy" manner. Hence, given the relatively small size of the IUE "large" aperture, it is quite credible that only a few stars might be included at a given pointing. Central to much of the work presented in this and the following papers in the series is the assumption that careful spatial decomposition of images acquired with the IUE SWP camera allows us to isolate the spectra of *individual* hot stars in the crowded cores. It was for just this purpose that the POLYSTAR procedure was developed.

(Earlier UV studies based on data from the OAO-2 and ANS satellites (refs) dealt with properties of *integrated* cluster light, because of their much larger apertures.) Because of its proven usefulness in this and other several other areas of IUE research, the POLYSTAR procedure is soon to be added to the Goddard RDAF library of standard analysis routines, where it will be available for use by visiting GOs (see Altner and Shore 1992). In this section we shall highlight those features of POLYSTAR which were used in the reduction of the M 79 LBL spectra. More detailed discussions can be found in Altner (1988*a*, 1988*b* and 1989).

The IUE "spatial axis" is nearly parallel to the long axis of the large aperture and almost perpendicular to the dispersion direction (hence, it is also called the cross-dispersion axis). The instrumental response to a point source in the cross-dispersion direction for the short wavelength spectrograph ranges between 4″.6 and 6″.0 (FWHM) under conditions of optimum focus (CBB). One can therefore expect to resolve discrete sources if they ~~are not too close together, by which we mean~~ have a separation ~~less~~ greater than 0.849 times the FWHM of the point-spread function (PSF). This ~~is based on~~ applies the Rayleigh criterion, ~~which specifies the minimum separation at which an analytical minimum might be found between~~ for two ~~peaks~~ objects of equal intensity. However, as we shall show, by making certain appropriate assumptions about the system it is sometimes possible to resolve point sources separated by distances smaller than the Rayleigh limit. The most convenient unit of measure for discussing the spatial resolution properties of IUE data is the "line", which represents the boundaries between diagonal pixels in the LBL files (Turnrose and Harvel 1980), or half diagonal pixels in the higher resolution extended-LBL (ELBL) format adopted by the IUE Observatory as of October 1, 1985 (Muñoz Peiro 1985). Based on the 1″.51/pixel plate scale derived by Panek (1982) for the SWP camera, we find that one line of an ELBL file spans 1.06 arcseconds.

The POLYSTAR program performs a simultaneous non-linear least-squares fit to the spatially resolved data, assuming there are N point sources in the large aperture. (A modified POLYSTAR approach has been used to separate point-like and extended sources, *e.g.*, see Reichert *et al.* 1988, but in this work all spatial components are considered to be stars, or unresolved clumps of stars.) The choice of N is clearly an important initial step, but it is not always a simple one, since an

improved fit can always be obtained by including an additional component (at least in the sense that the residuals always become smaller). Instrumental effects, such as poor focus or target drift in the aperture, may mislead one into believing that additional weak sources are present. This problem was discussed in some detail in Altner (1989), where is was shown that the F-test for the statistical significance of an extra component, combined with the requirement of "realistic" spectra, provide sufficient criteria from which one could chose a reasonable value of N. In Figure 2 we show the POLYSTAR fits to each spectrum, assuming four point sources in the aperture in each case, based on these criteria. The slightly broader profiles apparent in Figure 1 for SWP 28936 suggested a possible fifth component in this field of view, but the evidence for this was not compelling.

The cross-dispersion PSF in the large aperture of the SWP camera is best described as a "skewed gaussian", *i.e.*, a gaussian with a long asymmetric wing on the side toward the small aperture (Snijders 1980, CBB). Following CBB, we write the skewed gaussian function as

$$y(x) = \psi \exp\left\{ -\ln 2 \left[\frac{\ln[1 + 2\beta(x-\mu)/\gamma]}{\beta} \right]^2 \right\} \qquad \text{for } 2\beta(x-\mu)/\gamma > -1 \tag{1}$$

where

$$\gamma = \frac{\text{FWHM} \cdot \beta}{\sinh \beta} \tag{2}$$

and where

$$\text{FWHM} = 2\sqrt{2 \ln 2}\,\sigma \tag{3}$$

as it does for the symmetrical gaussian. The function defined in Eq. 1 is zero outside the specified limits. The parameter β measures the degree of asymmetry of the function. As $\beta \rightarrow 0$ the function reduces to the symmetrical gaussian.

A skewed-gaussian representation of the cross-dispersion profile thus requires four parameters to be determined for each of the N components. We attempt to fit the data with the function

$$Y = \sum_{j=1}^{N} y_j = f(\mu_1, \sigma_1, \psi_1, \beta_1, \mu_2, \sigma_2, \psi_2, \beta_2, \ldots, \mu_N, \sigma_N, \psi_N, \beta_N) \tag{4}$$

where μ_j is the location of the peak of the jth component, *i.e.*, its "center",

σ_j is the width of the jth component,

ψ_j is the amplitude, or peak value of the jth component, and

β_j is the dimensionless skew parameter of the jth component.

Since each of the fitting parameters is wavelength dependent, as discussed in Altner (1989), independent fits are obtained in several wavelength bins. Based on these fits, a relative fraction of the flux at each line is assigned to each component. These weighting factors are applied to all the samples in that bin, hence wide bins would naturally translate into large uncertainties in the resulting spectra. For the medium–good quality data we have obtained of M 79 we use bins 50 Å wide. POLYSTAR is set up to handle variable bin widths, should the signal-to-noise characteristics vary significantly across the spectrum (see, for example, Altner and Heap 1988).

The "best" fit, in the sense of the formal least-squares method, is that combination of parameters which yields the minimum χ^2. However, all of the parameters which describe the fitting function need not be *free* parameters. In order to take advantage of our knowledge of the instrumental properties which pertain to spatial resolution, or to incorporate spatial or spectral information we might have about the target itself, we have installed several options in the POLYSTAR code which allow control over the values of any one or more of the $4N$ parameters. In fact, in the present application both the width, σ, and the skewness factor, β, are prescribed functions of wavelength (based on results from CBB and Altner 1989, respectively), so the number of free parameters to be fit in each bin is $2N$. In addition, it is often useful to constrain the *separation* between a weak source and a strong or relatively isolated component, to enforce consistency in each bin. In practice, this is done by first allowing the centroids of all components to be determined in each bin. The mean separation between a strong component and one or more others is then derived, after rejecting obviously bad bins, and then is applied in a second pass over all bins. In this "fixed offset" option, the formal χ^2 of the fit is larger than for an unconstrained fit, but it is clearly superior to one in which the relative separation between two or more components is allowed to differ significantly from bin to bin. A similar approach was used to control the flux *ratio*, ψ_2/ψ_1, in a few of the IUE spectra used to identify SK-69 202 as the progenitor of SN 1987A (Sonneborn *et al.* 1987*b*).

Once the skewed gaussian profiles for each component are determined in a particular wavelength

bin they serve as "extraction slits" in the following sense. Each individual component profile is described by a set of array elements g_{jk} $(k = x_l, \ldots, x_r)$, where x_l and x_r are the user specified line numbers of the effective aperture, beyond which the the data is pure background noise—*e.g.*, $x_l = 40$ and $x_r = 70$ for SWP 25303 from Figure 1). We then define,

$$G_k \equiv \sum_{j=1}^{N} g_{jk} \tag{5}$$

such that,

$$f_{jk} = g_{jk}/G_k \tag{6}$$

is the relative weight of the jth component at line k. The above normalization condition implies that,

$$\sum_{j=1}^{N} f_{jk} = 1 \tag{7}$$

which is a statement of a kind of "conservation of flux" principle, in the sense that *all* of the flux at line k is distributed among the N components (POLYSTAR does not filter the data).

We employ the weights defined in Eq. ?? as multiplicative constants in the summation step in order to derive the net extracted spectrum. In the *standard* IUESIPS extraction of a point-source from the LBL (ELBL) file the data arrays are simply summed over 9 (18) lines. From this "gross" spectrum an appropriate mean background array, scaled to the proper slit width, is subtracted to obtain the net spectrum. In the case of aperture-filling, multiple sources, however, we derive the spectrum for component j by summing over the limits of the effective aperture, after multiplying by the derived relative weight:

$$\vec{F}_j = \sum_{k=x_l}^{x_r} f_{jk}(\vec{d}_k - \vec{b}) \tag{8}$$

where $\vec{d}_k$ is the gross spectrum at line k, and where $\vec{b}$ is the mean smoothed background array, normalized to one line. For an unblended point source this reduces to the IUESIPS standard extraction (if k_l and k_r are properly chosen), since the weighting factor $f_{1k} = 1$ for all k. We use vector notation in the above to denote quantities which are arrays along the *dispersion* direction. As the data in each bin is analyzed, the net extracted spectrum for each component in that bin is inserted into a storage array which holds the results of extractions in previous bins. After data

in the last bin has been processed and stored the complete spectrum can be retrieved for further analysis, along with the appropriate epsilon array. Data pertaining to the fits in each bin are stored in a separate file for later review, if necessary.

We identify three categories of uncertainty which may affect the final extracted spectra, namely *i*) the quality and reliability of the data, *ii*) the fitting procedure itself, and *iii*) the validity of assumptions incorporated into the procedure.

Factors affecting the reliability of the data, such as the effect of stray light from outside the aperture and light loss due to partial occultation by the aperture edges, are difficult to evaluate. Schiffer (1982) has estimated that a source contributes an amount proportional to $d^{-2.5}$, where d is the distance of the source from the center of the aperture ($40'' \geq d \geq 5''$). Carpenter *et al.* (1987) have studied the effects of diffraction spikes due to the mirror support structure. They concluded that significant extra flux is sometimes detected, depending upon the orientation of the large aperture with respect to the contaminating source. These effects are expected to be more important for extended sources than for point-like sources. The opposite problem of partial occultation can result in significant underestimates of the flux (see Altner 1988*b* and § 4). Particle hits both inside and outside the effective aperture region are treated by pre-filtering the data in the dispersion direction. This helps to avoid incorrect estimates of the background level and component weights. The use of wide bins to compensate for low signal-to-noise is an unavoidable source of uncertainty, but is not a severe problem in the featureless continuum regions. Very broad bins inevitably result in errors in the f_{jk} due to the curvature problem (Altner 1989) but the amount depends on the degree of separation between the components. Fortunately, this effect is easy to spot (if it is severe) and one or more of the constraints discussed above can usually be applied to a troublesome bin to correct the problem.

The second major source of uncertainty concerns the errors in the parameters reported by the POLYSTAR routine. These errors are a measure of the curvature of the χ^2 hypersurface in the words of Bevington (1969), being the diagonal elements of the error matrix. Bevington notes that the parabolic extrapolation used to approximate the curvature of the χ^2 hypersurface is somewhat

sensitive to the starting points used in the search procedure. The approximation is valid only if the starting points are close enough to the local minima that higher order terms in the expansion become truly negligible. Our experience confirms this point; we have noted occasions where the procedure did not converge within the (self-imposed) limit of ten iterations, whereupon a change in the initial guesses resulted in convergence. In practice, we always estimate the peak centers as closely as possible, using a cursor on a graphics terminal. Again, constraining the values of certain parameters always reduces the errors of the remaining free parameters, and often solves the convergence problem as well. This amounts to a confinement of the search algorithm to a restricted portion of the χ^2 hypersurface.

Lastly, let us consider several of the explicit assumptions in the procedure. For example, although the skewness parameter is clearly an important element in the analytical description of the instrumental PSF, it cannot realistically be left as a free parameter in the case of severely blended multiple profiles. Yet, the error bars in Altner's (1988*a*) mean β function are rather large. Weak sources are most susceptible to large errors in the extracted spectrum if the adopted mean skewness function is not truly representative, especially if they lie to the *right* (*i.e.*, at larger line number) of a strong source in the LBL data.

A related concern is the validity of the $\sigma(\lambda)$ function adopted from CBB. As already noted, both focus and telescope drift may broaden the PSF. Although several tests have shown that the focus correction algorithm included in POLYSTAR is probably valid for a given value of the focus STEP, we note that during a long exposure the STEP parameter can change and one unique value may not apply. It is possible to account for target drift by scaling the CBB σ function. Indeed, the images in Figure 1 suggest that such a step might be appropriate in the case of one of the M 79 spectra (SWP 28936). Instead, we have chosen to process all three spectra in a consistent manner, using the CBB function, since scaling is somewhat arbitrary and can sometimes cause more problems than it solves.

b) APS

From the individual stellar spectra obtained using the methods described in the preceding

section we wish to learn ~~something of the physical state of the stars. Ultimately, we are concerned with~~ the position of the stars in the log L, log T_{eff} or log g, log T_{eff} diagrams. Here we shall show that it is possible to obtain realistic, consistent values for the effective temperature, radius, luminosity, and surface gravity for the stars found within the aperture. The method we employ relies on the accuracy of the IUE absolute flux calibration and the validity of a grid of model stellar atmospheres. A well determined distance and reddening for each cluster is also required. The extent to which possible errors in these quantities affect our results is also discussed.

The model atmospheres which we compare to the extracted stellar spectra are those of Kurucz (1979 and unpublished). These models have been used before in a number of comparisons to Population II spectra (Huenemoerder, de Boer, and Code 1984, hereafter HBC; Cacciari *et al.* (1987); Nesci 1981). A thorough discussion of the shortcomings of the models when used in the study of Population II stars is given by Kurucz (1987). The model fluxes are converted to values found at the earth by multiplying by the factor $\pi(R/d)^2$ where R is the stellar radius and d is the stellar distance.

In estimating T_{eff} for these stars we use ~~what Böhm-Vitense (1981) calls an "indirect" method, that is~~, a comparison of the shape of the relative energy distribution of the stellar spectrum and the models. As Böhm-Vitense (1981) points out, ~~while~~ this method is not sensitive for very hot stars, but the steep intensity drop near 1600 Å in stars later than A2 makes the ultraviolet spectrum in this region a very sensitive indicator of effective temperature. Indeed, we find that in the temperature range 8,000 K–11,000 K the comparisons are fairly sensitive to our "best fit" criteria (to be described below), giving some confidence that the correct model temperature was chosen. The problem of temperature determination from the spectral slope is exacerbated by our necessary reliance on the limited spectral range covered by IUE SWP camera. With the much longer "lever arm" available by combining UBV colors with UV data it is fairly easy to distinguish a star with an effective temperature of, say, 18,000 K from one of 20,000 K using this method. However, optical colors are not available for the stars studied in this paper, hence the small change in the slope of the far UV continuum at high temperatures remains the fundamental limitation to the method. The lack of

LWP or LWR spectra is not serious, since tests show that in the vast majority of cases where both SWP and LWR(P) spectra were available to us (i.e., the IUE standard stars, field HB stars, and individual cluster UV-bright stars) the atmospheric parameters derived using the combined spectra were essentially the same as those found from the SWP spectra alone.

HBC showed from four-color photometry that $\log g$ was almost 0.5 dex smaller for the cooler field HB stars, compared to main sequence stars of the same temperature. Our experience confirms their result that the UV fluxes of the models are not gravity sensitive, especially for the hotter stars. Because of the logarithmic dependence of $\log g$ on the stellar mass and the small range of masses likely for stars on the horizontal branch, we were able to obtain credible estimates of the "actual" surface gravity (calculated on the basis of an assumed mass and the derived stellar radius). This provided a weak "self- consistency" criterion for choosing the most representative Kurucz model, in that we tended to favor those with $\log g$ not too different from the derived value, although this was not always possible.

The analysis in this paper and of those in the series to follow deals with SWP spectra, which isolates the hottest stars. In the temperature range 10,000 K–50,000 K only solar abundance models were computed by Kurucz. The use of the solar abundance models in a study of Population II stars is justified as follows. First, Cacciari *et al.* (1987) did not find good agreement between their HB stars and the Kurucz models, but their paper is mainly concerned with the cooler field HB stars. Of the 33 stars for which they were able to derive effective temperatures, 20 were cooler than 5,500 K and only 3 were hotter than 8,500 K. The hottest star in their sample (HD 85504, T_{eff} =10,000 K) was the only one of the 33 for which they actually did find a best fit (in the least-squares sense) using a solar abundance model. Moreover, they report that the "error" in T_{eff} and $\log g$ one would get by using solar versus 1/100th solar abundances is only about 200 K and 0.25 dex, respectively, for a star near 8,500 K. These errors are already considerably smaller than the combined uncertainties associated with our methods, and are smaller yet in the hotter stars. Second, HBC assumed, a priori, a value of log A = −1.0 for all 17 of their field HB stars (6 of which were in common with the Cacciari *et al.* 1987 sample), based on earlier abundance

analyses for a few of the objects. However, one of the conclusions of their study was that the metal poor models are too bright below 1600 Å, in complete agreement with our findings. HBC also found that while the normalized field HB fluxes shortward of 1800 Å were larger than those of Population I stars of approximately the same temperature (an effect presumably due to the lower metals in the Population II atmosphere), this effect decreased significantly as they compared hotter stars of both populations. For $T_{eff} \geq 10,000$ K this difference in the continuum shape is no longer noticeable. The clear separation between the Population I and Population II stars in their $C_{15\text{-}19}$ versus (b-y) diagram is widest for the cool stars and disappears at $T_{eff} \geq 10,000$ K. It is noteworthy that four of the hotter stars in the HBC sample (ranging in T_{eff} between 8,800 K and 15,300 K) were shown by Greenstein and Sargent (1974) to have an unusually strong Mg II 4481 Å line, reminiscent of Population I stars. Thus, it may be that these and other stars at the blue end of the HB are in a more advanced stage of evolution and that nuclear-processed material has been transported to the surface layers. Michaud, Vauclair, and Vauclair (1983) have shown that radiative diffusion, expected to be most important in the hotter HB stars, could be responsible for large overabundances of heavy elements, an effect apparently seen by Kodaira and Philip (1981) for blue HB stars in M4 and NGC 6397 and by Glaspey *et al.* (1989) and Crocker, Rood, and O'connell (1986) for blue HB stars in NGC 6752. This tendency of stars at the hotter end of the HB to be spectroscopically and photometrically indistinguishable from younger stars might also explain Tobin's (1987) observation of a number of apparently normal B stars at high galactic latitude.

By comparing the models to the absolutely calibrated, dereddened spectra extracted from the LBL data (and rebinned to the coarser resolution of the models) we can determine the radius of the star (Gray 1976, and references therein). Conservation of energy, in the absence of reddening, requires that

$$4\pi d^2 F(\lambda) = 4\pi R^2 \pi f(\lambda) \tag{9}$$

for which we can write

$$R(\lambda) = 4.43 \times 10^7 d \left(\frac{F(\lambda)}{\pi f(\lambda)} \right)^{\frac{1}{2}} \tag{10}$$

where, d is the distance to the star in parsecs, $F(\lambda)$ is the observed flux and $f(\lambda)$ is the model flux

at wavelength λ, and the stellar radius, R, is measured in units of solar radii. Of course, the idea is to obtain a result where R (λ) is the same at all points in the spectrum, since we expect any given star to have a unique and well determined photospheric size, independent of wavelength, over this small a wavelength interval. (It is possible to use the dispersion in the derived radius, as well as an "eyeball" comparison of the slope of the UV continuum of a model spectrum with that of the actual data, to assess which of several model atmospheres in a grid of models gives the best match.) In this way estimates of the stellar radius and effective temperature are obtained. Following this, the bolometric luminosity is found from the relation

$$\log \frac{L}{L_\odot} = 4 \log \frac{T}{T_\odot} + 2 \log \frac{R}{R_\odot}. \tag{11}$$

The approximate surface gravity is likewise easily obtained,

$$\log g = \log \frac{m}{m_\odot} - 2 \log \frac{R}{R_\odot} + 4.438 \tag{12}$$

where m is the mass of the star. Log g is fairly insensitive to the value of the mass adopted; a reasonable value for stars of the type we are considering is $m/m_\odot = 0.55 \pm 0.15$ (Sweigart, Mengel, and Demarque 1974; hereafter SMD). The uncertainty in $\log g$ associated with this range of masses is less than 0.15 dex, quite small when compared to the model grid spacing or other errors.

From the above we see that it is straightforward, at least in principle, to derive the stellar atmospheric parameters from the IUE spectra. In practice, several operations must be performed on the input spectra prior to comparing them to the model atmospheres. These operations include absolute calibration, correction for interstellar reddening, trimming to avoid spurious data at the extremities of the SWP camera's wavelength range, removing obviously bad data points, and, finally, binning the data to the coarser wavelength resolution of the models so that a 1:1 correspondence is established between points along the IUE and model spectra. The first two operations are typically done immediately following the POLYSTAR spatial decomposition; data files containing the absolutely calibrated, dereddened spectra are saved to disk. The ~~analyst~~ user later retrieves a given spectrum and decides which combination of trimming, weighting and smoothing is most appropriate to that spectrum. The binning operation is accomplished automatically within the APS routine

each time it is run. Pixels assigned zero weight are not used in the calculation of the bin means. In very noisy spectra this will sometimes result in a bin or bins containing nothing but zero-weighted points, in which case that portion of the spectrum is excluded from further consideration.

A radius is then calculated at each point in the spectrum, according to Eq. 10, using the chosen model and the processed input spectrum. Acceptance or rejection of a particular model as the best match to the input spectrum is thereafter based on several criteria, as mentioned above. An alternate, more statistically rigorous approach has been used by Cacciari *et al.* (1987). Not satisfied with the coarse Kurucz model grid spacing in T_{eff} and log g , they found least-squares fits by interpolating between existing models, as described in Malagnini and Morossi (1983). We considered doing something similar early in this work but rejected the idea because such an approach seemed unwarranted, given the combined uncertainties in the IUE data, the POLYSTAR decompositions, and the distance and reddening estimates. Also, least-squares fitting to the models may introduce additional uncertainties and/or numerical errors. Lastly, the models themselves may not be adequate, hence interpolating between them is of questionable value.

4. Results

Several lines of evidence suggest that the same objects appear in the large aperture in each of the three SWP spectra of M 79. First, as discussed in Appendix A, the center-of-light pointing in each case yields virtually the same right ascension and declination coordinates. Second, the distribution of light within the aperture, as shown in the LBL data of Figure 1, is also very similar. (Note that the pattern appears "flipped" in the middle spectrum, SWP 28936, relative to the other two. This is a consequence of its position angle, which differs from the others by approximately 180°.) Lastly, as we shall show below, the spectra of each of the components extracted via the POLYSTAR procedure agree very closely in all three images.

We show in Figure 2 the POLYSTAR fits to the three line-by-line images, summed over the wavelength interval 1650–1700 Å. Fits in this and other 50 Å-wide bins were used to determine mean component separations in each image, which were then applied in a second pass over the data, as described in § 3*a*. In each case the data were fit assuming that four components contibuted to the

Component	μ	σ_μ	ψ	σ_ψ
SWP 25303				
1	45.76	0.05	4.36E+04	7.74E+02
2	52.53	0.19	1.95E+04	1.25E+03
3	57.16	0.06	8.31E+04	1.24E+03
4	61.57	0.09	3.99E+04	1.24E+03
SWP 28936				
1	46.43	0.10	4.31E+04	1.49E+03
2	50.76	0.07	8.62E+04	1.43E+03
3	55.35	0.13	3.86E+04	1.35E+03
4	60.66	0.07	4.52E+04	1.04E+03
SWP 33152				
1	42.03	0.07	4.64E+04	1.11E+03
2	49.59	0.20	3.72E+04	3.06E+03
3	53.20	0.10	1.06E+05	2.53E+03
4	57.27	0.10	6.11E+04	2.34E+03

Table 2: POLYSTAR fits for the three SWP images of M 79 (1650–1700 Å). For each component we list the fitted centroid position (μ) with its 1σ error, and the peak value (ψ) with its 1σ error. In all cases the gaussian width (σ) was 2.02 lines, interpolated from the CBB function for this interval, and the skewness (β) was 0.21, interpolated from Altner's (1988*a*) function.

overall profile (shown by open circles). The individual component gaussians are shown as dotted lines and their sum by a thin, solid line. Residuals are shown by filled squares.

The parameters of the fits shown in Figure 2 are listed in Table 2, where the centroid positions and their 1σ uncertainties are in units of "line number", and the amplitudes and their 1σ uncertainties are in FN units. For convenience of notation we number the components left to right, with increasing line number. When we refer to these objects as 'stars", however, we reverse the numbering in the case of SWP 28936, to account for its nearly 180°position angle relative to the other two images. Hence, by Star 1 we mean the object contributing to Component 1 of SWP 25303 (or S25303C1), Component 4 of SWP 28936 (S28936C4), and/or Component 1 of SWP 33152 (S33152C1). Likewise, Star 3, the brightest object in the M 79 spectra, is S25303C3, S28936C2, and/or S33152C3. Mean separations used in the fixed-offset pass were applied relative to Star 1, clearly the most spatially distinct object in all three images.

The component separations derived from the various images are, of course, only projections of the stars' true positions along the IUE cross-dispersion axis. However, as pointed out by Altner

(1988*b*), with two or more observations at of the same field of view, obtained at different spacecraft roll angles, it is possible to derive true "two dimensional" sky positions of the stars in the field. Given the 21.1° difference in position angle between SWP 25303 and SWP 33152 and the derived mean component separations, we have employed this method to ascertain the relative coordiantes of the four stars on the sky, as shown in Figure 3. In this figure north is up, east is to the left, the stars are labeled by number as discussed above, and we have superimposed representations of the IUE large aperture, correct in scale and orientation but subject to slight ($\sim 2''$) uncertainties in centering (solid line for SWP 25303, dotted line for SWP 33152). The symbol sizes are meant to convey *qualitative* brightness differences. This figure reveals that both Star 1 and Star 4 are very close to an edge of the aperture in SWP 33152 whereas they fit "comfortably" within the aperture for SWP 25303. Indeed, as discussed below, both of these stars show slightly reduced flux levels in the later image, and partial obscuration may very well be the explanation (Altner 1988*b* shows how this effect could also have caused apparent variability among stars in the core of M15). A somewhat elongated "blob" of light is apparent in the far-UV image of the core of M 79 obtained with the UIT by Hill *et al.* (1991), of a scale and orientation consistent with the spatial distribution suggested by Figure 3, but this equivalence must be regarded as tentative until the UIT images are completely reduced (Hill, private communication).

INSERT In principle, a similar two-dimensional map could be generated using the orientations and separations of, say, SWP 25303 and SWP 28936. However, the spatial profiles for these two images in Figure 2 show that Star 1 is significantly closer to the other three objects in SWP 28936 than in the earlier image, much closer than the small roll angle difference (7°; 180° rotations merely reverse the pattern) could possibly account for. We have searched at length for a viable explanation for this observation (which, in fact, provided the motivation to obtain a third observation of this field) but no ready answer has emerged. That the *total* flux within the two apertures is the same provides an important constraint, suggesting that the same stars were observed in both cases. After much hair-pulling we are forced to conclude either that *a*) Star 2 is intrinsically variable, *b*) additional sources are present in the SWP 28936 image, partially filling in the gap between Star 1 and the

INSERT pp. 18-19

When the SWP 29936 image was taken, we noted that Star 1 appeared significantly closer (about 2" or 3σ) to the other three objects in the earlier image; the roll angle difference of 7° was insufficient to explain this anomaly. To check whether this represented a true physical motion of the star, we were motivated to obtain a third observation of the field, SWP 33152. In the third image, Star 1 appeared in the original location, within statistics. Since the total flux within the apertures are the same in all cases, and there is close agreement between the spectra of each individual observation of Star 1 (see Figure 4), we conclude that we are observing the same 4 objects in all 3 observations.

"clump" of three objects centered on Star 3, or *c*) that Star 1 is really outside the aperture in these images, thereby allowing a small relative rotation to have a big effect. Another possibility is based on recently unearthed pre-flight photographs of the IUE large apertures (SWP and LWP cameras; M. Perez, private communication). These photos show that the shapes of the large apertures are more rectangular than previously believed, and, perhaps most importantly, that the edges are not smooth but rather jagged, so that the light scattering characteristics of one end are not necessarily similar to those at the other end (*i.e.*, 180°rotations are *not* necessarily equivalent for stars near the edge). None of these explanations are particularly appealing, however, so we leave the question in an open state. We shall henceforth ignore the positional discrepancy, in the face of strong spectral evidence that the components are indeed the same star, but it is with considerable reluctance that we do so.

From the POLYSTAR fits to the profiles we extract the individual stellar spectra, as decribed in the previous section. In Figure 4 we display these spectra for each star, from each of the three images ('+', '∗', and '◇' for SWP 25303, 28936, and 33152, respectively). Because we are more interested in the overall shape of the continuum than in narrow spectral features, we have averaged the data in 50 Å-wide bins. The individual stellar spectra from each image are clearly similar, although there are minor differences. The biggest difference is the reduced flux level of S33152-S1 which, as suggested by the results of Figure 3, may be due to Star 1 being partially outside the aperture in this image. The other slight differences may be attributed to one or both of the following situations. First, slight broadening of the PSF compared to the CBB funtion used in the POLYSTAR fits, (due to drift of the target in the aperture during the long exposure) would be the major contributor to errors in the weighting factors assigned to each component. This would shift flux belonging to one component to be assigned to another (the "Peter-to-Paul" effect). In support of this possibility, we note that the the sum of the individual spectra is the same in both SWP 25303 and SWP 28936, and in SWP 33152 as well (if the flux for Star 1 is increased by about 40%, bringing it up to the level found in the first two images). Second, contributions from a large clump of cool giant stars may cause a slight excess in a spectrum at long wavelengths ($\lambda \geq 1650 Å$),

DERIVED PARAMETERS FOR THE M 79 CORE COMPONENTS

SWP	Star	T_{eff}	$R/R_\odot$	σ_R	$\log L/L_\odot$	$\log g$	V	B-V	N_{HB}
25303	1	12.0	2.6	10.5	2.12	3.3	15.7	-0.06	3-4
	2	10.0	3.4	15.5	2.02	3.1	15.5	-0.02	2-3
	3	12.0	3.6	6.6	2.39	3.1	15.0	-0.06	5-8
	4	11.0	3.3	6.9	2.17	3.1	15.4	-0.06	3-4
28936	1	12.0	2.6	5.3	2.10	3.3	15.7	-0.06	2-4
	..	10.0	3.8	8.5	2.12	3.0	15.3	-0.03	2-4
	3	12.0	3.4	4.8	2.33	3.1	15.2	-0.06	4-7
	4	11.0	3.6	7.8	2.22	3.1	15.2	-0.06	3-5
33152	1	TBD							
	2	TBD							
	3	TBD							
	4	TBD							
Co-added	1	TBD							
	2	TBD							
	3	TBD							
	4	TBD							
30951	L656	11.0	3.2	2.13	3.1	13.9	-0.22		
10170	II-48	12.0	3.4	2.32	3.1	13.9	-0.17		

finish ?

Table 3: Results derived by comparing the Kurucz (1979) models to the spatially resolved components in each IUE image. Column 3) effective temperature (in units of thousands of degrees K); column 4) stellar radius; column 5) uncertainty in the radius(%); column 6) logarithmic luminosity; column 7) log surface gravity; column 8) optical magnitude and column 9) color (both of which are deduced from the models, not from observation); column 10) number of single HB stars needed to account for the derived luminosity (see next section.

a contaminant which might be position angle dependent. Despite these small differences, we shall henceforth allow an exposure-time-weighted mean of the three observations to represent the final spectrum of each of the four stars.

5. Discussion

Throughout the analysis described above we have explicitly assumed that the four peaks observed in the cross-dispersion profiles represent those of single stars. Additional sources which might contribute non-negligible flux to the observed signal come in two flavors: those spatially distinct from the four we have identified, and those so close to one or more of the four that they are unresolvable with the IUE. As described in Altner (1989), the F-test provides an unbiased estimate of the likelihood that additional stars of the first kind are present. Applied to the M 79 profiles, the F-test rejected a fifth component in SWP 25303 and SWP 33152 and was inconclusive in SWP 28936, so we forged ahead using $N = 4$ in the POLYSTAR procedure. Any other stars which may have actually been present were ignored, and the fluxes assigned to the four stars are

therefore upper limits. Contributions of the second kind are more insidious, since a dense clump of several stars may masquerade as one source, resulting in a large error in the derived luminosity of the presumed single star. This uncertainty is especially severe in clusters whose core radius subtends a small angle, *i.e.*, the most distant or the most compact globulars.

One way that we have approached the issue of single stars vs small clumps of stars is to derive realistic estimates of how many stars should have been included within the area of the IUE large aperture, based on the cluster's properties, and compare that with how many sources were actually observed. We employ the luminosity of one blue HB star as a convenient unit of brightness. To estimate how many HB stars are expected to fall within the aperture we use King's (1962) empirical scaling law for the brightness profile of the nuclear region of a globular cluster, *i.e.*,

$$f(r) = f_o/(1 + r^2/R_c^2), \tag{13}$$

where R_c is the core radius and f_o is the central surface brightness. Expressing R_c in arcseconds and f_o in magnitudes per square arcsecond, we define a "luminosity density" profile (solar luminosities per square arcsecond) as

$$l(r) = l_o/(1 + r^2/R_c^2), \tag{14}$$

where $l_o = 100^{\Delta M/5}$ and $\Delta M = 4.83 + 5\log d - 5 + A_v - f_o$. Under the assumption that the center of the large aperture and the peak in the King (1962) model coincide, and that the King model is a valid description of the nuclear region ~~in the first place~~, integrating the luminosity profile over the dimensions of the IUE aperture gives the number of solar-type stars expected. Dividing this result by 500 yields the estimated number of red giants within the aperture, since the typical luminosity of a red giant is $\sim$ 500 $L_\odot$ (Buonanno *et al.* 1981). Finally, if it is true that the number of HB stars in a typical cluster is 0.8–1.0 times the number of red giants (Iben 1972), this then gives us the approximate number of HB stars within the aperture, predicted from cluster properties and the King model, which we will call $N_{\rm King}$.

For M 79, with R_c = 10.5 arcseconds, f_o = 16.27 visual magnitudes per square arcsecond, d = 13.0 kpc and E(B-V)=0.01 (Webbink 1985) we find that $N_{\rm King}$ = 14. This is probably an upper limit, since the core radius of M 79 was determined from *optical* concentric aperture photometry,

while the UV spatial distribution (which is really what concerns us here) is likely to be much more sharply peaked, as found by Dupree *et al.* 1979 in other clusters. Another reason to treat $N_{\rm King}$ as an upper limit in this case is that Djorgovski and King (1986) found M 79, among others, to have a "possibly collapsed" core, as indicated by a slight central brightness excess, or "cusp". Although the King model is not strictly valid in cusp clusters, it should nevertheless provide a useful order-of-magnitude estimate for the expected number of stars, given the small central excess in M 79.

As a measure of the number of HB-equivalent stars actually observed we take

$$N_{\Delta L} = L_{obs}/L_{\rm HB} \tag{15}$$

where $L_{\rm HB}$ is the theoretical HB luminosity at the same effective temperature as the UV source, and L_{obs} is the luminosity derived from fits to the Kurucz models, described in the previous section, for each star (see Table 3). Unfortunately, this method requires that the HB be ***strictly*** horizontal, while Sweigart (1987) has shown that the slope of the HB depends upon the intitial core helium abundance and the time elapsed since the bluest stars reached the ZAHB. We bracket the available range by using Sweigart's ZAHB model with Y=0.20 and Z=0.0001 as an upper limit to $N_{\Delta L}$, and his evolved sequence with Y=0.30 and Z=0.0001 as a lower limit to $N_{\Delta L}$. Finally, we define $N_{\rm total}$ as the sum, over all resolved sources in the aperture, of the calculated $N_{\Delta L}$ for each source. $N_{\rm total}$ is therefore equivalent to the total number of HB stars *observed* within the aperture. For M 79, $N_{\rm total}$ =11–20 HB stars, for Sweigart's evolved and ZAHB models, respectively.

Both methods, one based on cluster properties and the other on observed flux, suggest that there should be about a dozen HB stars contained within the large aperture at the central core of M 79. Although this number is small (among the 20 clusters studied by Altner 1988*a*, $N_{\rm King}$ ranged between 1 and 144), it is still a factor of three larger than the number of spatially distinct "components" used in the POLYSTAR fits. In other words, *each* of four stars listed in Table 3 would have to actually be a tight clump of about 2–4 stars, if we consider them to be HB stars. We describe below why we consider ~~Instead, we consider~~ it much more likely that each is a single star approximately 2–4 times more luminous than an HB star. ~~As outlined below~~, If correct this means that these stars are probably in a post-HB

stage of evolution.

With the possible exception of the blue stragglers, all hot stars in globular clusters are thought to have passed through a phase in which they evolve away from the main sequence after exhaustion of hydrogen in the core, and subsequently climb the red giant branch during H-shell burning. The onset of He-core burning, with significant and rapid mass loss from the cool outer envelope, then transforms a red giant into an HB star. The residual envelope mass and metallicity are the most important parameters in determining the color of the newborn (zero-age) HB star (ZAHB), with the blue ones having the smallest and most metal-poor envelopes. Model calculations beyond the zero-age HB (*e.g.*, see SMD) suggest that the hottest HB stars eventually evolve through the subdwarf channel and become white dwarfs, while the cooler, intermediate-mass HB stars have sufficient envelope mass to sustain both H-shell and He-shell burning as they evolve redward toward the asymptotic giant branch (AGB, also known as the "second giant branch"). We shall follow the nomenclature of SMD in calling these "supra-HB" stars.

The highest mass HB stars ($M \approx 0.65 M_\odot$), which are found at the red end of the ZAHB, never cross through the supra-HB region, but rather evolve directly upward along the AGB (Zinn 1974). So, whereas ZAHB stars of very low mass, such as the $0.51 M_\odot$ model of SMD, populate the supra-HB but never quite reach the AGB, higher mass stars, such as their $0.6 M_\odot$ model, can *only* populate the post-AGB sequences. Intermediate masses will pass through the supra-HB region before climbing the AGB. Significant mass loss occurs as these star evolve toward higher luminosity along the AGB (Renzini 1981*a*, Schönberner 1983). Stars in this stage of evolution are still double-shell sources, with the hydrogen burning shell providing upwards of 90% of the luminosity. A number of thermal pulses may occur, in which products of He-shell burning are dredged up to the surface layers, and a final pulse, perhaps accompanied by severe mass loss in a "superwind" (Renzini 1981*b*), terminates the AGB phase. Post-AGB stars then begin a quiescent, blueward evolution at constant luminosity (Paczynski 1970). Schönberner (1983) has modeled the transition of AGB stars into hot remnants, namely the central stars of planetary nebulae (CPN).

The post-HB fate of a star thus depends critically on its mass. The supra-HB stars, constituting

a sequence about 1–2 magnitudes above the HB, are directly linked to the low- and intermediate-mass, blue end of the HB. Their spectra are very similar to that of HB stars. The larger mass HB stars, however, eventually become high-luminosity post-AGB stars, survivors of turbulent and sometimes explosive helium shell flashes, rapid and variable mass loss, and possible convective mixing, leading to chemical abundance anomalies in some cases (Gingold 1974). Hot supra-HB and post-AGB stars found in globular clusters are often collectively called "UV-bright" stars (Zinn 1974).

Many of the known UV-bright stars were first reported as a distinct class of objects by Zinn, Newell, and Gibson (1972; ZNG). They were discovered (well outside the cluster cores) by a technique of blinking U and V plates. A comprehensive listing of globular cluster UV-bright stars is included in Harris, Nemec, and Hesser (1983). A few of these stars are O-type subdwarfs and one is the central star of a planetary nebula (K648 in M15). These stars are bright enough to significantly affect the integrated light of a stellar population, if they occur in sufficient numbers, a point stressed by Renzini and others in a number of papers (*e.g.*, see Renzini 1981*b* and Greggio and Renzini 1990). But the rapid evolutionary timescale for these stars makes them quite rare—there are only 46 *confirmed* UV-bright stars in 36 galactic globular clusters (de Boer 1985). Determining the true frequency of occurrence of these stars, by finding additional candidates hidden in the crowded cores, was one of the major goals of the IUE globular cluster program. By matching both the spectral distributions and luminosities to known supra-HB stars we shall now show that several of the M 79 core sources are newly-discovered supra-HB stars.

In Figure 5 we compare the co-added spectra of Star 1 and Star 3 extracted from the spatially resolved profiles of the three M 79 IUE images (thin solid lines), with stars in M13 (dotted lines) and the respective Kurucz (1979) models which best fit the stellar continua (heavy solid lines). In both panels the fluxes of the M13 stars were scaled only by the square of the cluster distance ratio, so it is clear that the M13 and the M 79 stars are similar in luminosity as well as in spectral type. The two M13 stars were identified as UV-bright stars in the ZNG survey. L656 (also known as ZNG-6) was first discussed by Ludendorff (1905) and II-48 (ZNG-2) is among the stars in the

catalog of Arp (1955). Both are confirmed cluster members and were classified as Group I by ZNG (bluer than the Cepheid instability strip). L656 lies approxiamtely 1 arcmin from the cluster center while II-48 is 2 arcmin out, so both are beyond the 50″ core radius (Webbink 1985) in uncrowded regions. Properties derived for these two stars, using methods described earlier, are included in Table 3 for ease of comparison with the M 79 stars.

The very close agreement in both temperature and luminosity (and hence in radius and log g as well) between the M 79 core stars and the M13 stars is yet another argument in favor of interpreting at least these two M 79 sources as individual stars. Taken at face value, these results suggest that the core of M 79 contains at least two, and perhaps four new examples of the supra-HB class of UV-bright stars. While not nearly as rare as post-AGB stars (with lifetimes as short as 10^{-5} years these stars are extremely rare), hot supra-HB stars are rare enough that finding four new examples within the core may be significant. Among the 100 stars detected in the UIT near- and far-UV images of M 79 (at distances greater than 40″ from the center) about a dozen are a magnitude or so brighter than the HB and so might be considered as supra-HB stars (Hill *et al.* 1991). However, all of these are cool, with B-V ¿ 0.1; they found no hot post-HB stars. Neither did Cordoni and Auriere (1983), who compiled a CMD based on B and V magnitudes of 116 stars in a $1' \times 1'$ field at the center of M 79. (Although they did detect six stars with B-V ¡ 0., all appear to be HB stars. However, overcrowding may have prevented them from finding the stars we have detected with IUE within 20″ of the center.)

A ~~knee-jerk reaction to~~ finding more examples of ~~any~~ phenomenon inside a cluster core than outside of it is to invoke the crowded conditions that exist there to suggest that collisions or tidal captures have occurred. In this case, it is certainly possible that one or more of the stars may be binary in nature, but, as we have seen at least in the case of Star 3, two stars is not enough to explain the luminosity. Perhaps some other property of the core region gives rise to an environment more favorable to the existence of a larger number of post-HB stars inside than outside the core. A mass segregation mechanism which concentrates the more massive stars toward the core, *i.e.*, by gravitational "settling" would indeed have this effect since, as we have seen above, it is only

the intermediate- and high-mass HB stars which are able to evolve into supra-HB and post-AGB stars, leading one to naturally expect a larger number of stars in advanced stages of evolution to be found in the core.

Another segregation mechanism which would have the same effect was suggested by Buonanno *et al.* (1986) to explain an apparent an asymmetry in the radial distribution of the sdB stars in NGC 6752. From statistically complete photographic photometry of more than 5000 stars observed within in an inner annulus (1.'5–4.'5) and an outer annulus (4.'5–10′) they found that the spatial distribution of the bright (V< 15.5) HB stars generally showed a pattern of declining number with increasing distance from the center, similar to that of other cluster members (such as the sub-giants). On the other hand, the distribution of the fainter HB stars (V> 15.5) was flatter (no decline) an effect also observed in M15. (Our IUE observations of 9 spectra at or just outside the central core in NGC 6752, described in Paper II, resulted in non-detection of the faint but hot sdB stars, consistent with this trend.) As a working hypothesis, Buonanno *et al.* (1986) suggested that this effect arose due to a "spin-orbit" coupling which may originate during the early phases of star formation in dense clusters. Thus, proto-stars which were originally concentrated toward the center are ejected with increased rotation rates, which leads eventually to an increased core mass. This later results in an increased He-flash luminosity, and subsequently larger mass loss from the outer envelope. Once distributed in this fashion the sdB stars would be more prone to escape the cluster entirely as it made its periodic passages through the galactic plane, explaining the much greater number of sdB stars found in the halo population relative to the globular clusters. That NGC 6752 is believed to be a cluster in the post-core-collapse state strengthens the likelihood of this interpretation (Djorgovski and King 1986) of the spatial distribution of sdB stars in this cluster.

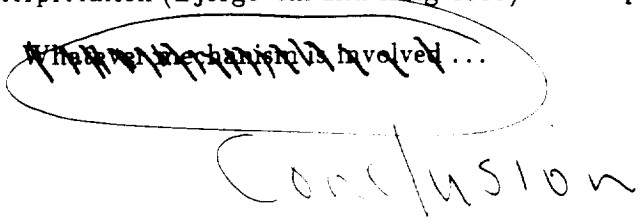

Conclusion

Whatever mechanism is involved, it would be useful to identify these stars optically. Using a narrow-band blue (or UV) filter, it should be possible to isolate these objects from red giants that dominate the cluster core. This analysis is vital for identifying the optical counterpart of the X-ray source associated with NGC 1904. ~~it is likely that one of the~~

We acknowledged Tad Pryor and ..... for helpful discussions. This work was supported in part by NASA Grant NAG 5-1750 and ...

Appnedix A: Post-Observation Determination of Target Coordinates

Observers using the IUE to obtain spectra of extended objects frequently supply the telescope operator with a target position that is sufficient to put the object within the field of view of the Fine Error Sensor (FES), and then interactively determine the "center of light" position by placing a cursor on the brightest FES pixel. The coordinates on the observing script, which eventually end up in the IUE image database, are therefore not very useful for determining precisely where the telescope was pointed during the observation. However, it *is* possible to reconstruct the precise pointing of the spacecraft, based on records of maneuvers that were executed at the time of the observation. In this Appendix we shall describe how this is done and shall demonstrate the process with the example of SWP 25303, our first spectrum of the core of M 79.

We wish to determine the actual equatorial coordinates of the observed stars. The maneuvers which take the satellite from an offset star to the target provide a *relative* position; from the known position of the offset star we can then obtain the true absolute position of the target. (A detailed discussion of the characteristics and operation of the FES camera can be found in Sonneborn *et al.* 1987*a*.) Here we need only emphasize that acquisition of bright but extended targets is usually accomplished by first selecting a star brighter than 12th magnitude with well known coordinates and proper motion as an "offset star". The satellite is slewed to the position of this star, which is then identified on the 10′.8 square FES image display. Using the target coordinates provided by the guest observer, a small offset maneuver is executed in order to bring the target into the FES field of view. If the target is bright enough (brighter than $14^m.0$) and reasonably compact, it is then placed at the FES reference point and a standard slew is performed to center it in the proper aperture. The resolution of the FES in this "prime mode" is nominally 0″.25, for targets falling at the center of its field. (The FES raster grid is known to be affected by geometric distortions. Targets falling near the edge of the FES field are subject to positional uncertainties as large as 3″.)

It is currently standard policy of the IUE Observatory that a record of every spacecraft slew is automatically scrolled to a line printer at the telescope operations center, and this information is later copied to microfiche. The position of the offset star is recorded in this "event list" in

units of arcseconds along the pitch (P) and yaw (Y) axes (see Figure 7). We transform these to FES coordinates (x, y), relative to the reference point, as follows (A. Holm, C.L. Imhoff, private communication):

$$\begin{pmatrix} x \\ y \end{pmatrix} = \begin{pmatrix} -1.770 & 3.286 \\ -3.364 & -1.812 \end{pmatrix} \begin{pmatrix} P \\ Y \end{pmatrix} \tag{16}$$

The separation between the offset star and the reference point in units of arcseconds is given by

$$\begin{pmatrix} \Delta\alpha \\ \Delta\delta \end{pmatrix} = \begin{pmatrix} -c_x \cos\theta & c_y \sin\theta \\ -c_x \sin\theta & -c_y \cos\theta \end{pmatrix} \begin{pmatrix} \Delta x \\ \Delta y \end{pmatrix} \tag{17}$$

where θ is the angle between the negative Y axis and the north direction and c_x =0.2680, c_y =0.2617 are the scale factors, in arcseconds per FES pixel, along the x and y axes, respectively.[1] Here $\Delta x = x$ and $\Delta y = y$ since the position of the offset star is already specified relative to the FES reference point.

The absolute FES coordinates of the target are also recorded in the event list and we again use Eq. 17 to transform these into a relative separation with respect to the reference point. The *total* separation between the offset star and the target is then the vector sum of the relative separations. Combining this with the equatorial coordinates of the offset star yields the true coordinates of the target. Note that in converting the relative coordinate separations into an absolute target position we must first take into account the "scale factor" between units of time and units of arc. That is, at a declination δ we have,

$$\Delta\alpha^s = \frac{\Delta\alpha''}{15\cos\delta} \tag{18}$$

where the superscripts refer to seconds and arcseconds, respectively.

As an example, consider the case of SWP 25303. The coordinates given to the telescope operator at the time of observation were $\alpha = 5^h22^m$, $\delta = -24°34'$ (Sawyer-Hogg, 1974). We used the $8^m.8$ star SAO 170395 as the offset star. With coordinates of $\alpha = 5^h22^m13^s.018$, $\delta = -24°44'0''.85$ (after correction for proper motion) SAO 170395 was a reasonable choice for an offset star, being only about ten arcminutes from the cluster (see Sonneborn *et al.* 1987*a* for a discussion of the correlation of large maneuver errors with large slew distances). The roll angle at the time of observation was

[1]The actual FES coordinate system is slightly distorted from this idealised description. Errors of 1–3″ are associated with these geometric effects, which become more pronounced at large distances from the origin.

105° 3′. The event log informs us that SAO 170395 needed a +50″.11 maneuver along the pitch axis and −355″.9 along the yaw axis in order to be brought to the reference point, while the (x, y) coordinates of the interactively determined center of light were $(-544, 664)$. Thus, from Eqs. 16 and 17 we find that SAO 170395 was 140″.9 east and 330″.7 south of the reference point, while the center of light was determined to be 68″.8 east and 259″.6 north (see Figure 7). Combining these we see that our target position was 72″.1 west and 590″.3 north of SAO 170395. After applying Eq. 18 to these figures we obtain a final position of $\alpha = 5^h22^m7^s.73$, $\delta = -24°34'10''.55$. The uncertainty in this position is estimated to be ±2″ in both right ascension and declination. These coordinates for the center of light of M 79 are quite close to those given by Webbink (1985), *i.e.*, $\alpha = 5^h22^m8^s$, $\delta = -24°34'12''$. Our second "center-of-light" observation of this cluster almost eighteen months later (SWP 28936) yielded a position of $\alpha = 5^h22^m7^s.62$, $\delta = -24°34'10''.30$, while the position for SWP 33152 was determined to be $\alpha = 5^h22^m7^s.44$, $\delta = -24°34'10''.00$, both in excellent agreement with that of SWP 25303. This agreement, of course, is the result of M 79 having a well defined center of light, and it is vital to our contention that the four stars observed in both of these images are the same.

Unfortunately, calculations such as the one described here for M 79 are not possible for *all* of the center-of-light images of globular clusters obtained with the IUE, since they depend on the availability of records of the spacecraft maneuvers. This information was only sporadically kept in the early days of the project, so there remains a degree of uncertainty in the meaning of "center of light" in a number of cases. Of course, this problem is not confined to globular cluster research, but is common to all extended source images for which exact coordinates were not specified by the guest observer. Those individuals responsible for preparing the final IUE data archive are duly concerned about the limitations that this places on the value of these images to researchers in the years ahead.

REFERENCES

Altner, B. and Shore, S. N. 1992, *NASA IUE Newsletter,* in press.

Altner, B. 1988a, PhD. Thesis, Rutgers University.

Altner, B. 1988b, in *A Decade of UV Astronomy with the IUE Satellite,* Vol. 2, p. 189.

Altner, B. 1989, *NASA IUE Newsletter,* **37**, 43.

Altner, B. and Heap, S. R. 1988, in *A Decade of UV Astronomy with the IUE Satellite,* Vol. 2, p. 257.

Altner, B., and Matilsky, T. A. 1984, *Pub. A.S.P.,* **96**, 783.

Arp, H. 1955, *A. J.,* **60**, 317.

Aurière, M., Adams, S., and Seaton, M. J. 1983, *M.N.R.A.S.,* **205**, 571.

Aurière, M., and Cordoni, J.-P. 1983, *M.N.R.A.S.,* **205**, 571.

Bevington, P. R. 1969, *Data Reduction and Error Analysis for the Physical Sciences*, McGraw-Hill, New York.

de Boer, K. S., and Code, A. D. 1981, *Ap. J. (Letters),* **243**, L33.

de Boer, K. S. 1985, *Astr. Ap.,* **142**, 321.

Böhm-Vitense, E. 1981, *Ann. Rev. Astr. Ap.,* **19** , 295.

Buonanno, R., Castellani, V., Corsi, C. E., and Fusi Pecci, F. 1981, *Astr. Ap.,* **101**, 1.

Buonanno, R., Caloi, V., Castellani, V., Corsi, C. E., Fusi Pecci, F., and Gratton, R. 1986, *Astr. Ap. Suppl. Ser.,* **66**, 79.

Cacciari, C. 1985, *Astr. Ap. Suppl. Ser.,* **61**, 407.

Cacciari, C., Malagnini, M. L., Morossi, C., and Rossi, L. 1987, *Astr. Ap.,* **183**, 314.

Caloi, V., Castellani, V., and Galluccio, D. 1984, in *Proceedings of the 4th European IUE Conference,* 497.

Carpenter, K., Stencel, R., Pesce, J., Brown, A., Judge, P., and Jordan, C. 1987, *NASA IUE Newsletter,* **33**, 20.

Cassatella, A., Barbero, J., and Benvenuti, P. 1985, *Astr. Ap.,* **144**, 335 (CBB).

Code, A. D. 1982, *Advances in Space Research,* **2**, 119.

Cordoni, J.-P., and Aurière, M., 1983, *Astr. Ap. Suppl. Ser.,* **54**, 431.

Crocker, D. A. Rood, R. T., and O'connel, R. W. 1986, *Ap. J. (Letters),* **309**, L23.

Djorgovski, S., and King, I.R. 1986, *Ap. J. (Letters),* **305**, L61.

Dupree, A. K., Hartmann, L., Black, J. H., Davis, R. J., Matilsky, T. A., Raymond, J. C., and Gursky, H. 1979, *Ap. J. (Letters),* **230**, L89.

Gingold, R. A. 1976, *Ap. J.,* **204**, 116. **USE 1974 ref?????**

Glaspey, J. W., Michaud, G., Moffat, A. F. J. and Demers, S. 1989, *Ap. J.,* **339**, 926.

Gratton, R. G., and Ortolani, S. 1986, *Astr. Ap. Suppl. Ser.,* **65**, 63.

Gray, D. F. 1976, *The Observation and Analysis of Stellar Photospheres*, Wiley, New York, p. 366.

Greenstein, J. L., and Sargent, A. I. 1974, *Ap. J. Suppl.,* **28**, 157.

Greggio, L., and Renzini, A. 1990, *Ap. J.,* **364**, 35.

Grindlay, J.E. 1981, **TBD??**

Grindlay, J.E. 1982, in *Galactic X-ray Sources*, Sandford, P. W., Laskarides, P., and Salton, J., eds., Wiley & Sons, p. 363.

Harris, H. C., Nemec, J. M., and Hesser, J. E. 1983, *Pub. A.S.P.,* **95**, 256.

Hill R.S., Greason M.R. and Hill J.K. *et al.* 1991, *B.A.A.S.,* **23**, 947.

Huenemoerder, D. P., de Boer, K. S., and Code, A. D. 1984, *A. J.,* **89**, 851. (HBC)

Iben, I. 1972, in *Dudley Observatory Report No. 4, The Evolution of Population II Stars,* A. G. Davis Philip, ed., p. 1.

King, I. R. 1962, *A. J.,* **67**, 471.

Kodaira, K., and Philip, A. G. D. 1981, in *IAU Colloquium No. 68, Astrophysical Parameters for Globular Clusters*, A. G. Davis Philip and D. S. Hayes, eds., p. 153.

Kurucz, R. L. 1979, *Ap. J. Suppl.*, **40**, 1.
Kurucz, R. L. 1987, in *IAU Colloquium No. 95, The Second Conference on Faint Blue Stars*, A. G. Davis Philip, D. S. Hayes, and J. W. Liebert, eds., p. 129
Ludendorff, ?? 1905, *Potsdam Publ.*, **15**, no. 50.
Malagnini, M.L., and Morossi, C. 1983, in *Statistical Methods in Astronomy*, ESA SP-201, 27.
Michaud, G., Vauclair, G., and Vauclair, S. 1983, *Ap. J.*, **267**, 256.
Muñoz Peiro, J. R. 1985, *NASA IUE Newsletter*, **27**, 27.
Nesci, R. 1981, *Astr. Ap.*, **99**, 120.
Paczynski, B. 1970, *Acta Astronomica*, **20**, 47.
Panek, R. J. 1982, *NASA IUE Newsletter*, **18**, 68.
Reichert, G. A., Wu, C.-C., and Filippenko, A. 1988, in *A Decade of UV Astronomy with the IUE Satellite*, Vol 2., p. 307.
Renzini, A. 1981*a*, *IAU Colloquium No. 59, Effects of Mass Loss on Stellar Evolution*, C. Chiosi, R. Stalio, eds., Reidel, p. 319.
Renzini, A. 1981*b*, Ann. Phys. Fr., **6**, 87.
Sawyer-Hogg, H. 1973, *Publications of the David Dunlap Observatory*, **3**, No. 6.
Schiffer, F. H. 1982, IUE internal memo.
Schönberner, D. 1983, *Ap. J.*, **272**, 708.
Snijders, M. A. 1980, *SERC IUE Newsletter*, No. 5, p. 85.
Sonneborn, G., Oliverson, N. A., Imhoff, C. L., Pitts, R. E., and Holm, A. V. 1987*a*, *NASA IUE Newsletter*, **32**.
Sonneborn, G., Altner, B., and Kirshner, R. P. 1987*b*, *Ap. J. (Letters)*, **323**, 35.
Strom, S. E., Strom, K. M., Rood, R. T., and Iben, I., Jr. 1970, *Astr. Ap.*, **8**, 243.
Sweigart, A. V., Mengel, J. G., and Demarque, P. 1974, *Astr. Ap.*, **30**, 13 (SMD).
Sweigart, A. V. 1987, *Ap. J. Suppl.*, **65**, 95.
Thompson, R. W. 1985, in *Record of IUE Three-Agency Coordination Meeting*, Computer Sciences Corporation, CSC/TM-84/6173, pp. A-229.
Tobin, W. 1987, in *IAU Colloquium No. 95, The Second Conference on Faint Blue Stars*, A. G. Davis Philip, D. S. Hayes, and J. W. Liebert, eds., p. 149.
Turnrose, B. E., and Harvel, C. A. 1980, *IUE Image Processing Information Manual*, NASA TM-79/6301.
van Albada, T. S., de Boer, K. S., and Dickens, R. J. 1981, *M.N.R.A.S.*, **195**, 591.
Webbink, R. F. 1985, in *IAU Symposium No. 113, Dynamics of Star Clusters*, J. Goodman and P. Hut, eds., Reidel, Dordrecht, p. 541.
Welch, G. A., and Code, A. D. 1980, *Ap. J.*, **236**, 798.
Zinn, R. J., Newell, E. B., and Gibson, J. B. 1972, *Astr. Ap.*, **18**, 390. (ZNG)
Zinn, R. J. 1984, *Ap. J.*, **193**, 593.

FIGURE CAPTIONS

Figure 1. Pseudo-color montage of the three SWP line-by-line iamges, showing similar multiple-source flux distribution in each field of view. The intensities have been scaled to maximize the contrast in flux interval from just above the noise to the level at 1350 Å. The correction for camera sensitivity has not yet been applied. Note the "reversed" orientation of SWP 28936 with respect to the other two. The bright ovals centered at 1216 Å show the shape and size of the large aperture, illuminated by the glow of geocoronal Ly-α emission.

Figure 2. POLYSTAR fits in the interval 1650–1700 Å for the three IUE spectra of M 79 shown in Figure 1. In all three panels the open circles represent the data after removal of the background, the solid line represents the overall fit to the data (*i.e.*, the sum of the individual skewed gaussians (shown as dotted lines for each component), and the filled squares represent the residuals (data – fit).

Figure 3. "Star map" generated by combining the derived gaussian centroid positions of the four sources in both SWP 25303 and SWP 33152, using the method described in Altner (1989). The SWP large aperture for each image is shown at the proper scale and orientation (solid line for SWP 25303 and dotted line for SWP 33152), subject to uncertainties of about 2″ in the absolute position of the center. Note that stars numbered 1 and 4, which are comfortably within the aperture for SWP 25303, are very close to the edge in the latter observation. From this evidence, and the observed decrease in flux for Star 1 in SWP 33152 relative to SWP 25303 (see Figure 4), it seems likely that Star 1 was partially outside the large aperture in the latter image.

Figure 4. Binned spectra for each component (star) derived from the three SWP spectra ('+', '*', and '◇' for SWP 25303, 28936, and 33152, respectively). With minor exceptions, the agreement is excellent and suggests, along with the spatial information derived from the line-by-line data, that the same four sources were observed in each image. The anomalously low flux for Star 1 in SWP33152 is probably due to its extreme proximity to the edge of the aperture (see Figure 3). A bin width of 50 Å was used in all cases.

Figure 5. Comparison of extracted spectra in the core of M 79, based on a exposure-time-weighted average from all three SWP images, to known UV stars in M13 and Kurucz models. Upper panel: the "isolated" star (Star 1) in M 79 (thin solid line) versus the star L656 in M13 (SWP 30950/30951; dotted line), and a Kurucz model with T_{eff} =11,000K, $\log g$ =3.5 (heavy solid line). Lower panel: the brightest star (Star 3) in the M 79 spectra (thin, solid line) versus the star II-48 in M13 (SWP 10170; dotted line), and a Kurucz model with T_{eff} =12,000K, $\log g$ =3.0 (heavy solid line). The spectra of the M13 stars have been scaled by the squared ratio of the distances to the clusters $(d_{M13}/d_{M79})^2$ = ([7.1 kpc]/[13.0 kpc])^2 = 0.30), suggesting that the intrinsic luminosities and gravities, as well as the temperatures, are nearly identical to the M 79 stars in both cases. The Kurucz models have been scaled as per Eq. ??.

Figure 6. The relative positions of the offset star SAO 170395 and the globular cluster M 79 in the FES plane as reconstructed from data pertaining to the image SWP 25303. The coordinate system is centered at the FES reference point, and the fiducial tickmark is expressed in FES units.

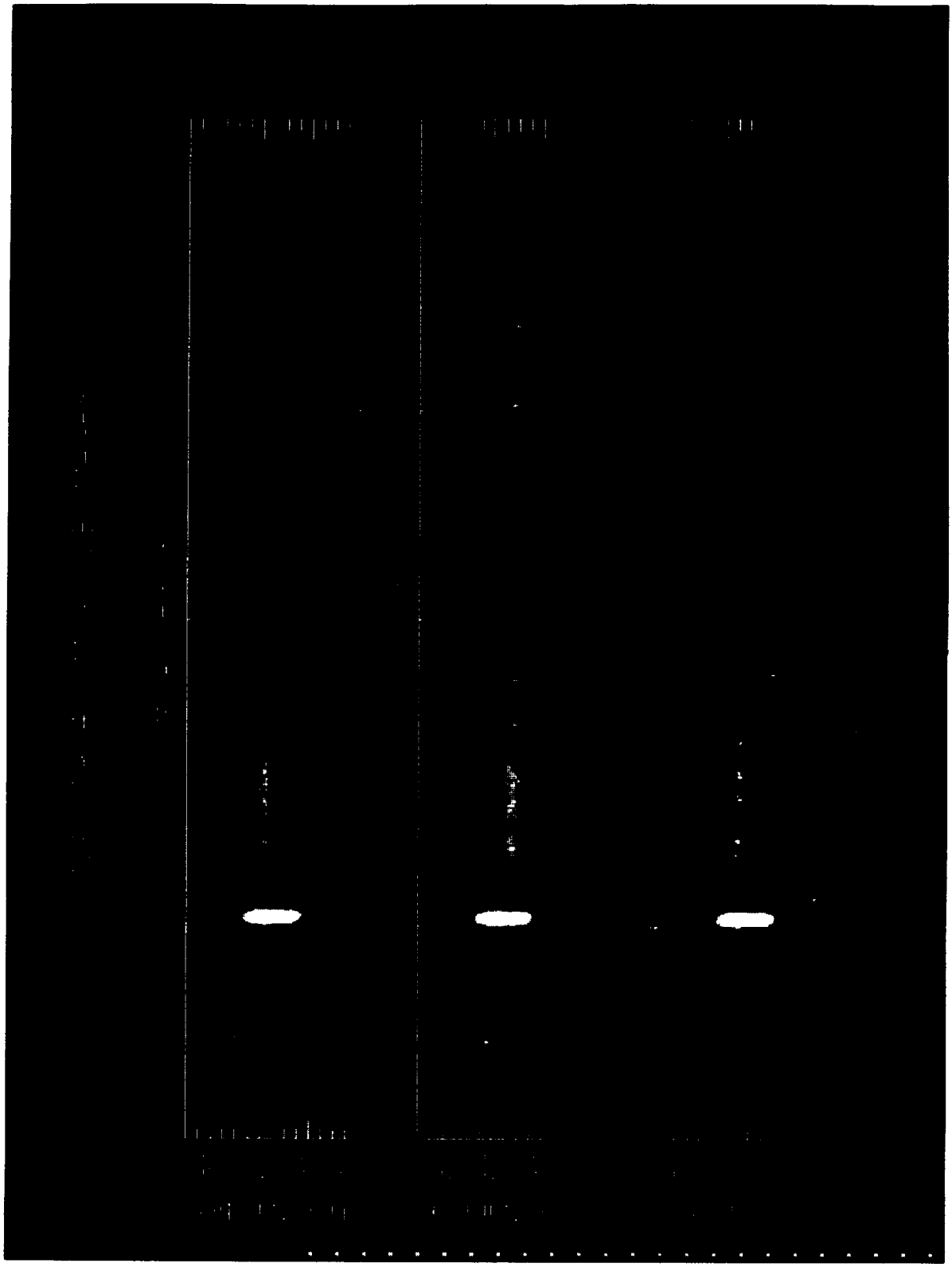

Fig. 1

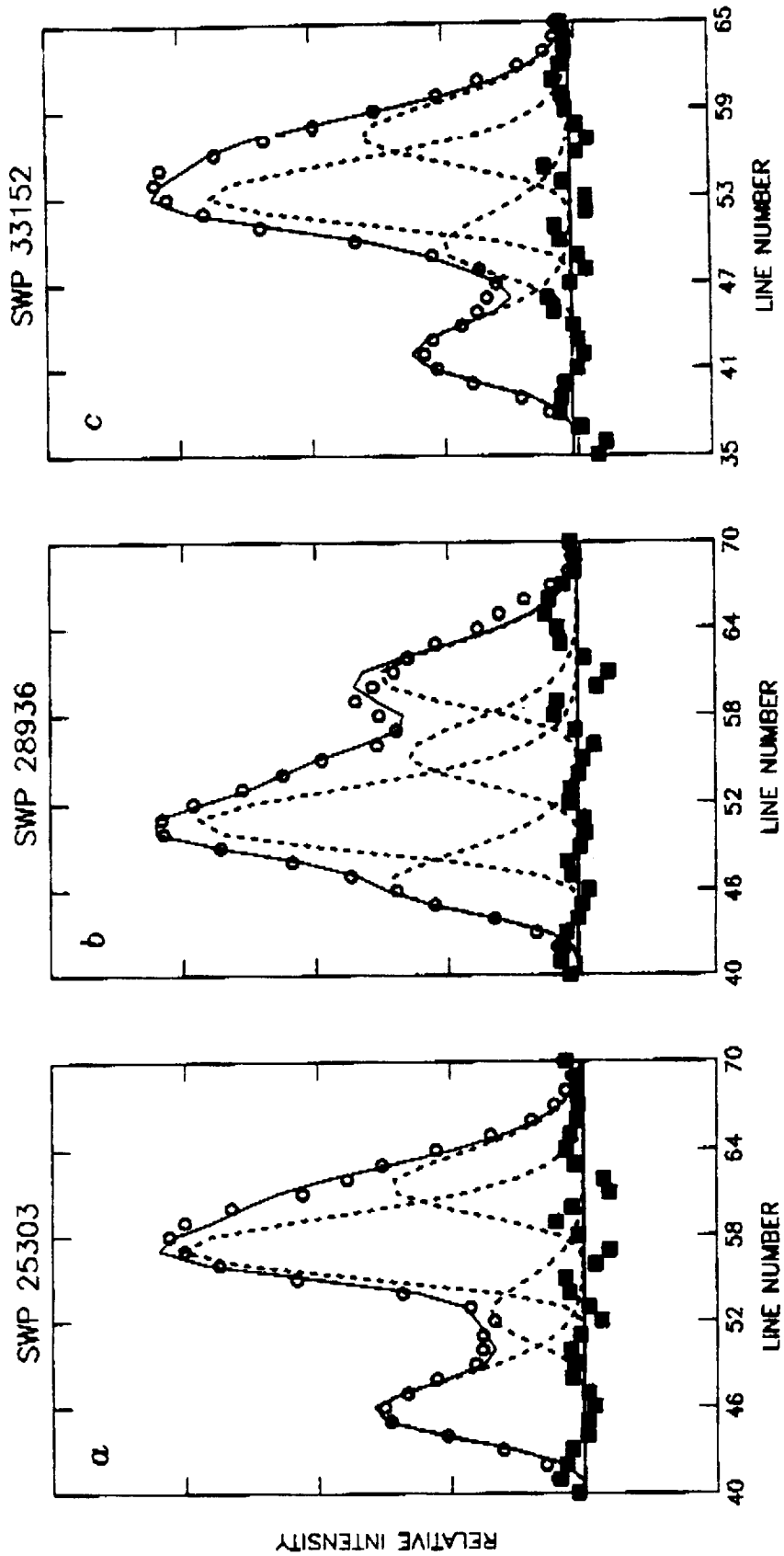

1650-1700 Å Figure 2

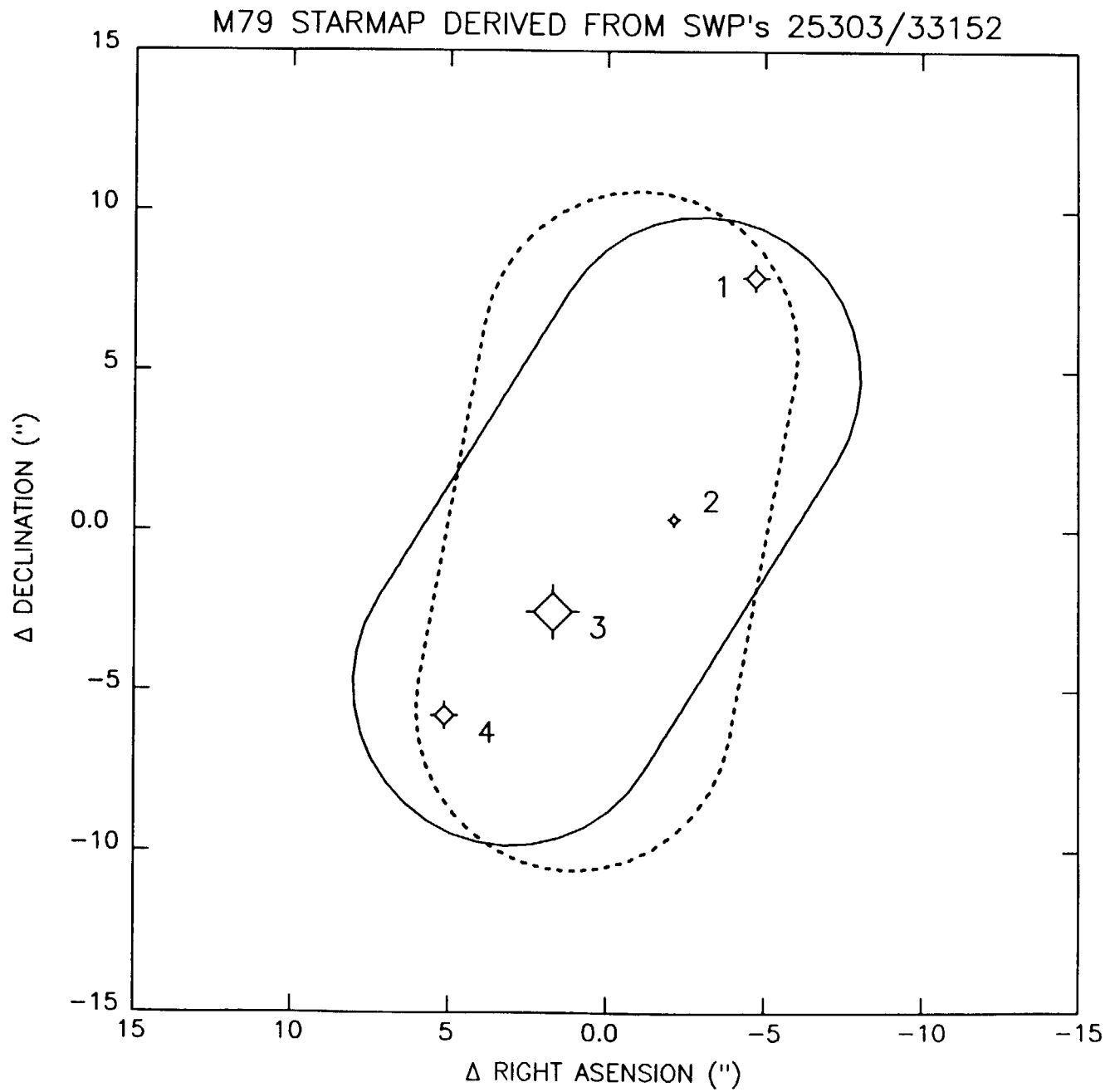
M79 STARMAP DERIVED FROM SWP's 25303/33152
15
10
5
0.0
−5
−10
−15
Δ DECLINATION (")
15
10
5
0.0
−5
−10
−15
Δ RIGHT ASENSION (")
1
2
3
4

Fig. 3

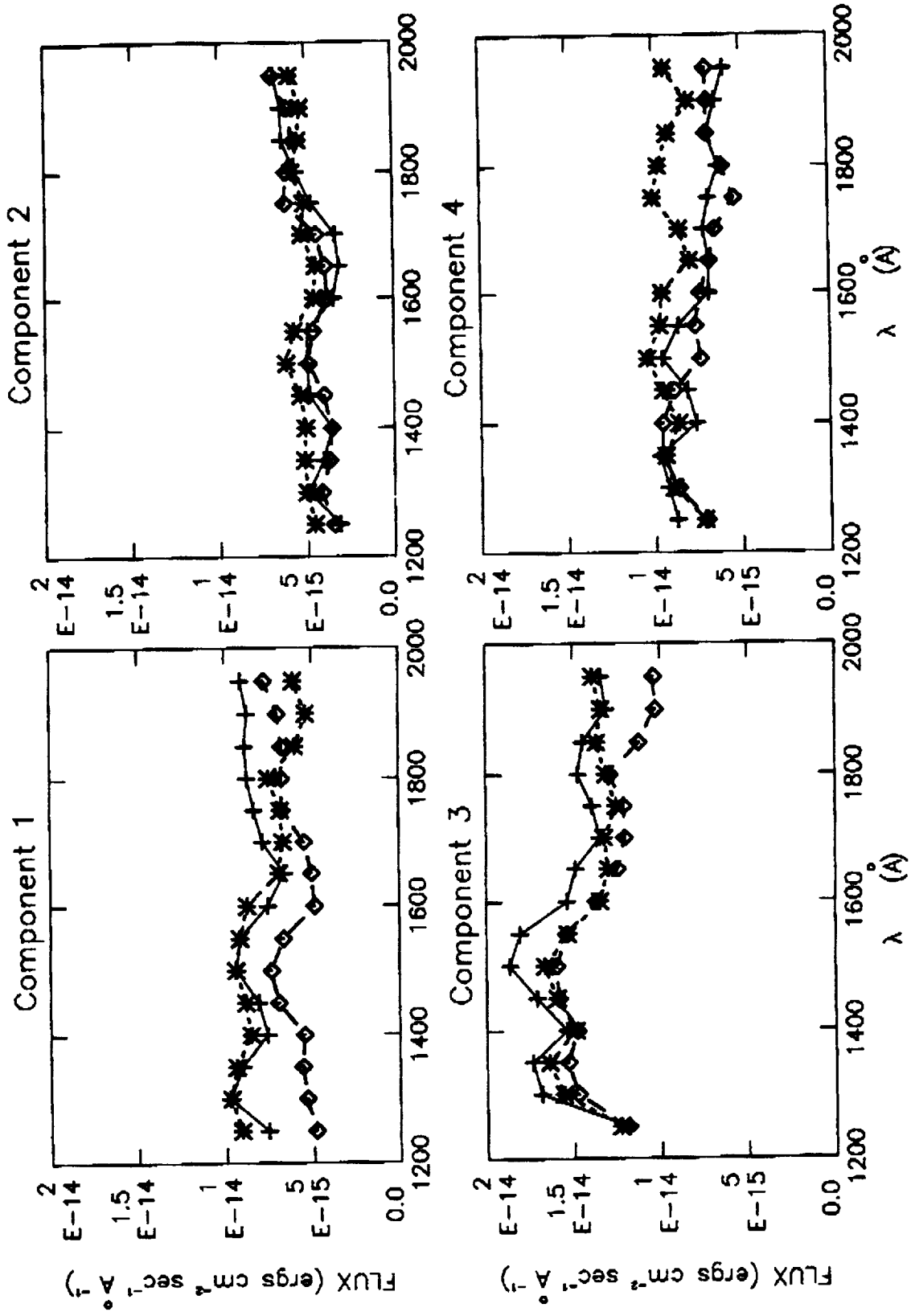

Fig. 4 [illegible] . Terms -mato slight changes due to processing

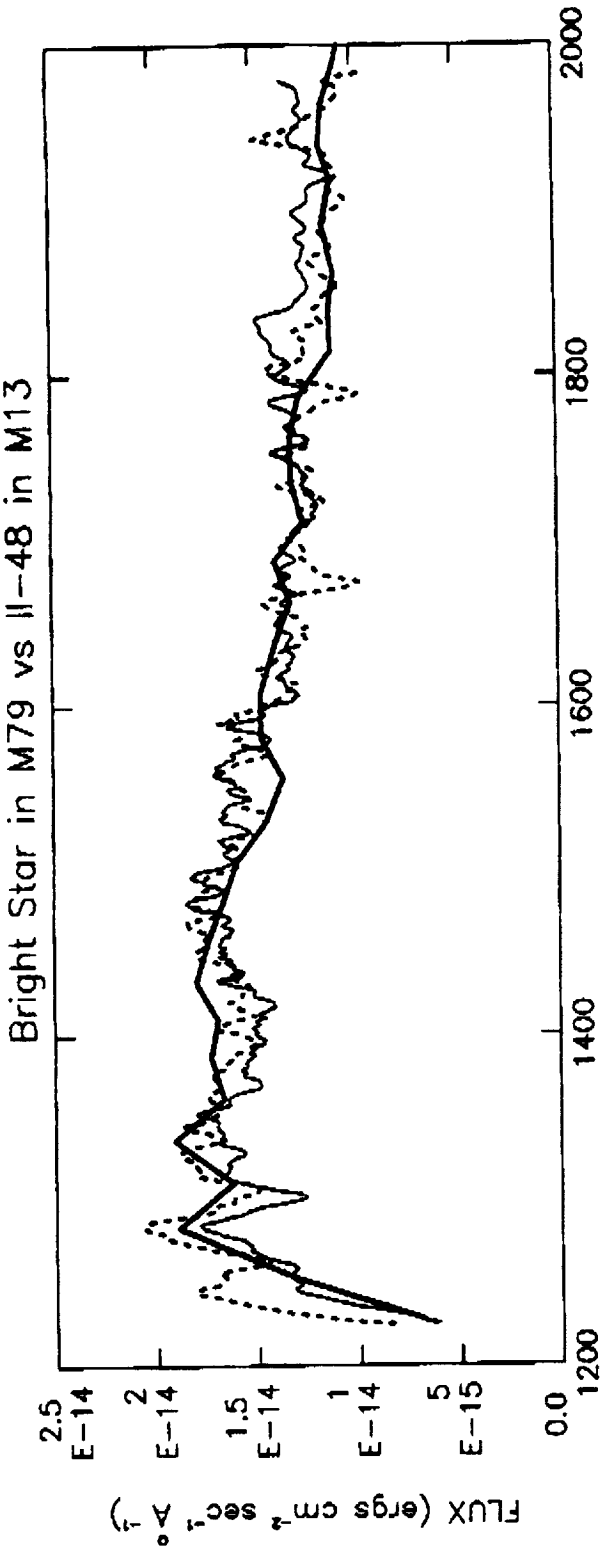

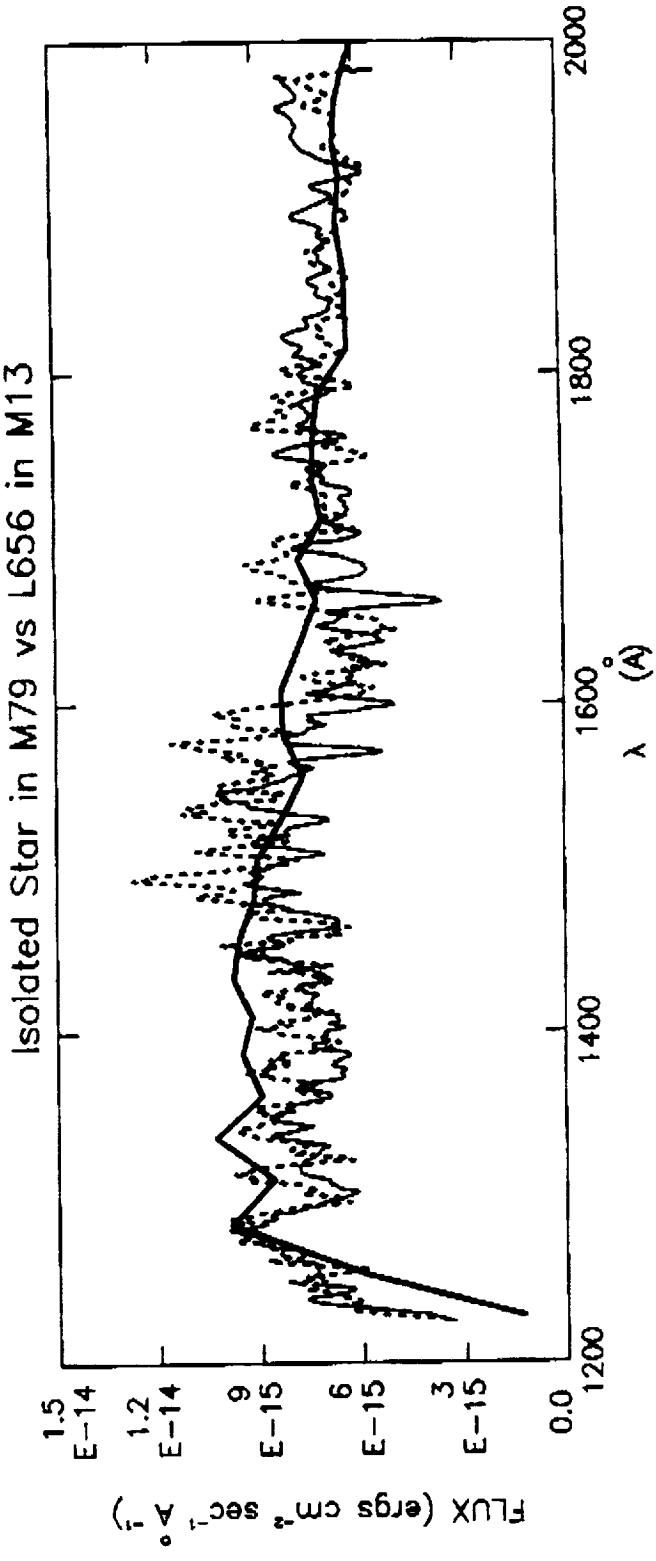

Aller & Mathis Figure 5